Fermi National Accelerator Laboratory

FERMILAB-Conf-98/168

Some Issues on the RF System in the 3 GeV Fermilab Pre-Booster

K.Y. Ng

Fermi National Accelerator Laboratory
P.O. Box 500, Batavia, Illinois 60510

June 1998

Published Proceedings of the *Workshop on Space Charge Physics in High Intensity Hadron Rings*, Shelter Island, Long Island, NY, May 4-7, 1998

Operated by Universities Research Association Inc. under Contract No. DE-AC02-76CH03000 with the United States Department of Energy

Disclaimer

Distribution

Some Issues on the RF System in the 3 GeV Fermilab Pre-Booster

K.Y. Ng

Fermi National Accelerator Laboratory,[1] *P.O. Box 500, Batavia, IL 60510*

Abstract. Some issues are presented on the rf system in the future Fermilab pre-booster, which accelerates 4 bunches each containing 0.25×10^{14} protons from 1 to 3 GeV kinetic energy. The problem of beam loading is discussed. The proposal of having a non-tunable fixed-frequency rf system is investigated. Robinson's criteria for phase stability are checked and possible Robinson instability growth is computed.

I INTRODUCTION

The proposed future Fermilab pre-booster has a circumference of 158.07 m. It accelerates 4 bunches each containing 0.25×10^{14} protons from kinetic energy 1 to 3 GeV [1]. Because of the high intensity of the beam, the problems of space charge and beam loading must be addressed. A preliminary rf system has been proposed by Griffin [2]. Here, we wish to examine the issues of beam loading and Robinson instabilities. We first present a possible resonant ramp curve with space-charge distortion of the rf waveform compensated. Then the rf system which will eliminate most of the transient beam loading is reviewed. We next consider the possibility of non-tunable rf cavities and the possible Robinson instabilities that follow. We find that the Robinson growth in synchrotron amplitude is small and the high-intensity Robinson phase-stability criterion is well satisfied.

II THE RAMP CURVE

Because of the high beam intensity, the longitudinal space-charge impedance per harmonic is $Z_\parallel/n|_{\rm spch} \sim -j100\ \Omega$. But the beam pipe discontinuity will contribute only about $Z_\parallel/n|_{\rm ind} \sim j20\ \Omega$ of inductive impedance. The space-charge force will be a large fraction of the rf-cavity gap voltage that intends to focus the bunch. A proposal is to insert ferrite rings into the vacuum chamber to counteract this space-charge force [3]. An experiment of ferrite insertion was performed at the Los Alamos Proton Storage Ring and the result has been promising [4]. Here we assume such an insertion will over-compensate all the space-charge force leaving behind about $Z_\parallel/n|_{\rm ind} \approx j25\ \Omega$ of inductive impedance. It may be a good idea to over-compensate the space charge, because an inductive impedance will help bunching so that the required rf voltage needed will be smaller.

---

[1] Operated by the Universities Research Association, Inc., under contract with the U.S. Department of Energy.

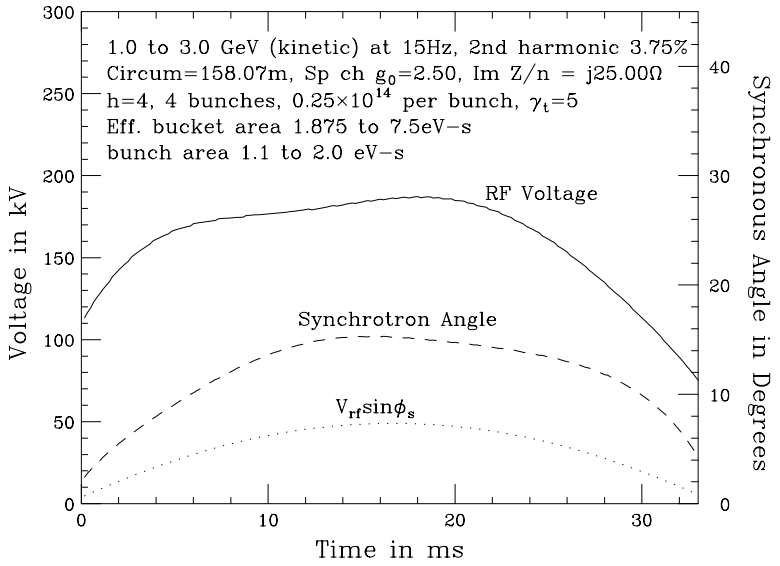

FIGURE 1. A typical ramp curve for the future Fermilab pre-booster.

The acceleration from kinetic energy 1 to 3 GeV in 4 buckets at a repetition rate of 15 Hz is to be performed by resonant ramping. In order to reduce the maximum rf voltage required, about 3.75% of second harmonic is added. A typical ramp curve is shown in Fig. 1, which will be used as a reference for the analysis below. This fraction of second harmonic was chosen because, in the present choice of initial and final bucket areas and bunch areas, raising this fraction beyond 3.75% will only flatten the rf gap voltage in the ramp but will not decrease the maximum significantly.

III THE RF SYSTEM

According to the ramp curve in Fig. 1, the peak voltage of the rf system is $V_{\rm rf} \approx$ 185 kV. Griffin proposed 10 cavities [2], each delivering a maximum of 18.5 kV. Each cavity contains 30 cm of ferrite rings with inner and outer radii 20 and 35 cm, respectively. The ferrite has a relative magnetic permeability of $\mu_r = 21$. The inductance and capacitance of the cavity are $L \sim 0.61$ μH and $C \sim 820$ pF. Assuming an average ferrite loss of 134 kW/m^3, the dissipation in the ferrite and wall of the cavity will be $P \sim 15$ kW. The mean energy stored is $W \sim 0.15$ J. Therefore each cavity has a quality factor $Q \sim 459$ and a shunt impedance $R_s \sim$ 12.5 kΩ. One such cavity is shown in Fig. 2.

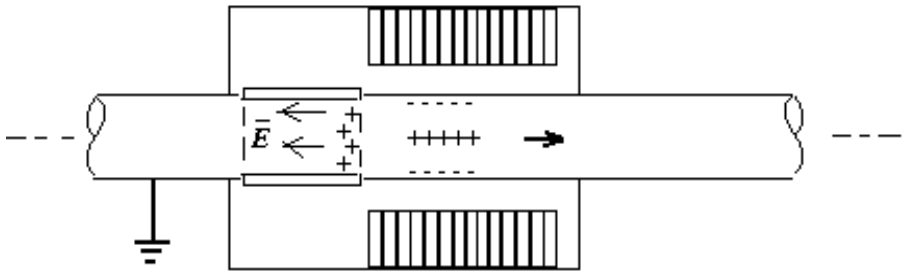

FIGURE 2. A ferrite-loaded cavity with a dielectric gap in the beam pipe. Protons move to the right.

Because each bunch contains $q = 4.005$ μC, the transient beam loading is large. For the passage of one bunch, 4.005 μC of negative charge will be left at upstream end of the cavity gap. Since another negative image current will start from the downstream end of the cavity gap following the bunch, an equal amount of positive charge will accumulate there, as illustrated in Fig. 2. Thus a voltage V_{t0} will be created at the gap opposing the beam current. For a short bunch, this transient beam loading voltage can have a maximum of

$$V_{t0} \sim \frac{q}{C} = 5.0 \text{ kV} , \tag{3.1}$$

where $C = 820$ pF is the gap capacitance. We note from Fig. 1 that the accelerating gap voltages at both ends of the ramp are only about or less than 10 kV in each cavity. If the wakes due to the bunches ahead do not die out, we need to add up the contribution due to all previous bunch passages. Assuming a loaded quality factor of $Q_{_L} = 45$, we find from Appendix C that the accumulated beam-loading voltage can reach a magnitude of $|V_t| = 37$ kV when the detuning angle is zero.

Griffin suggested to use a feed-forward system [2], which will deliver via a tetrode the same amount of negative charge to the downstream end of the gap so as to cancel the transient beam loading. This is illustrated in Fig. 3.

A feed-forward system is not perfect and we assume that the cancellation is 85 %. For a δ-function beam, the component at the fundamental rf frequency is 56.0 A. Therefore, the remaining image current across the gap is $i_{\rm im} = 8.4$ A. To counter this remaining 15% of beam loading in the steady state, the cavity must be detuned by the angle (see Appendix A)

$$\psi = \tan^{-1}\left(\frac{i_{\rm im}\cos\varphi_s}{i_0}\right) , \tag{3.2}$$

where φ_s is the synchronous angle and $i_0 = V_{\rm rf}/R_s$ is the cavity current *in phase* with the cavity gap voltage $V_{\rm rf}$. For high quality factor of $Q = 459$ which is accompanied by a large shunt impedance, the detuning angle will be large. Corresponding

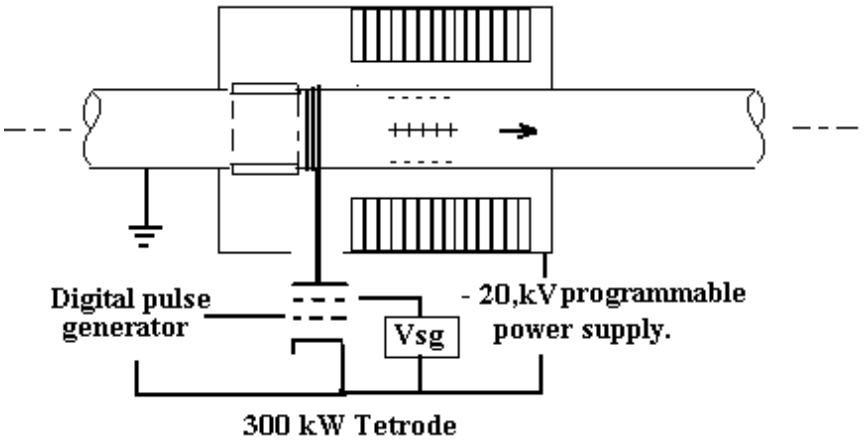

FIGURE 3. Transient beam-loading power tetrode connected directly to a rf cavity gap.

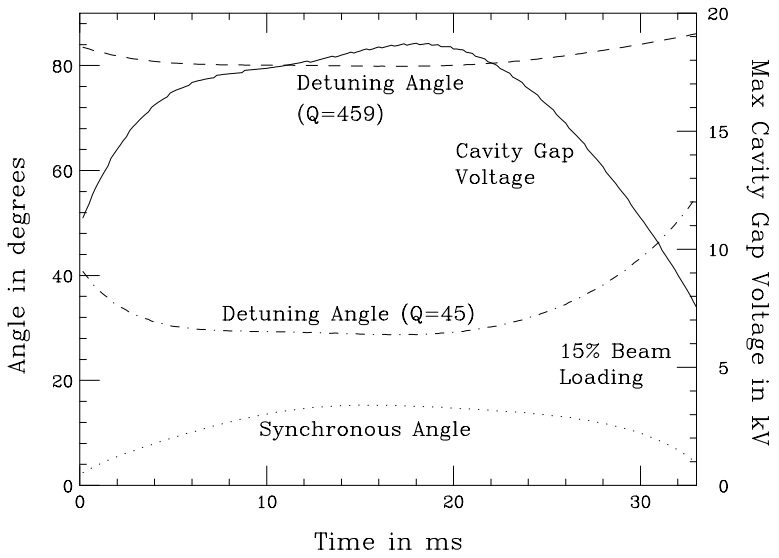

FIGURE 4. Detuning angle for the high $Q = 459$ and low $Q_{_L} = 45$ situations.

to the ramp curve of Fig. 1, the detuning angle is plotted as dashes in Fig. 4 along with the synchronous angle and maximum cavity gap voltage. We see that the detuning angle is between 80° and 86°, which is too large. If a large driving tube is installed with anode (or cathode follower) dissipation at ~ 140 kW, the quality factor will be reduced to the loaded value of $Q_{_L} \sim 45$ and the shunt impedance to $R_s \sim 1.22$ kΩ. The detuning angle then reduces to $\psi \sim 29°$ at the center of the ramp and to $\sim 40°$ or $\sim 56°$ at either end. This angle is also plotted in Fig. 4 as a dot-dashed curve for comparison. Then, this rf system becomes workable.

IV FIXED-FREQUENCY RF CAVITY

Now we want to raise the question whether it is possible to have a fixed resonant frequency for the cavity. A fixed-frequency cavity can be a very much simpler device because it may not need any biasing current at all. Thus the amount of cooling can be very much reduced and even unnecessary. It appears that the resonant frequency of the cavity should be chosen as the rf frequency at the *end* of the ramp, or $f_{_R} = 7.37$ MHz so that the whole ramp will be immune to Robinson's phase-oscillation instability [5]. However, the detuning will be large. For example, at the beginning of the ramp where $f_{\rm rf} = 6.39$ MHz, the detuning angle becomes $\psi = 85.2°$. Since the beam-loading voltage $V_{\rm im}$ is small, the generator voltage phasor $\tilde{V}_g$ will be very close to the gap voltage phasor $\tilde{V}_{\rm rf}$. As a result, the angle θ between the gap voltage $\tilde{V}_{\rm rf}$ and the generator current phasor $\tilde{i}_g$ will be close to the detuning angle, as demonstrated in Fig. 5. For example, Fig. 6 shows that, at the beginning of the ramp, the detuning angle is $\psi = 85.2°$. Although the total power delivered by the generator

$$\tfrac{1}{2}\tilde{i}_g \cdot \tilde{V}_{\rm rf} = \frac{V_{\rm rf}^2}{2R_s} + \tfrac{1}{2} i_{\rm im} V_{\rm rf} \cos\varphi_s \tag{4.1}$$

is independent of θ, the energy capacity of the driving tube has to be very large.

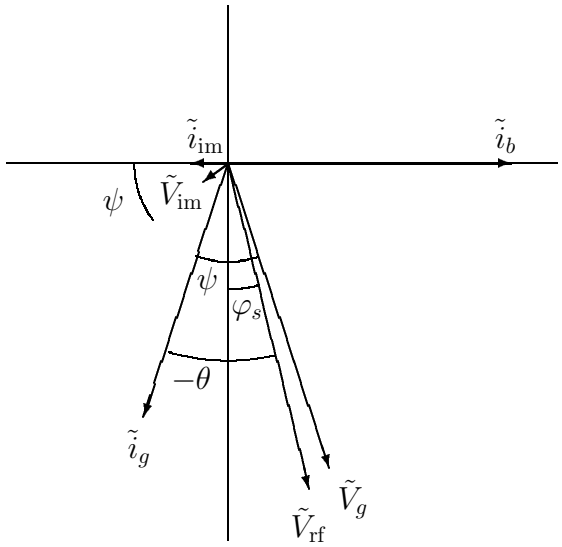

FIGURE 5. For a fixed cavity resonant frequency, the detuning angle ψ is fixed at each ramp time. When beam-loading is small, the angle θ between the gap voltage $\tilde{V}_{\rm rf}$ and the generator current $\tilde{i}_g$ will be close to ψ and will be large.

Another alternative is to choose the resonant frequency of the cavity to be the rf frequency near the *middle* of the ramp. Then the detuning angle ψ and therefore the angle θ between $\tilde{V}_{\rm rf}$ and $\tilde{i}_g$ will be much smaller at the middle of the ramp when the gap voltage is large. Although θ will remain large at both ends of the ramp, however, this is not so important because the gap voltages are relatively smaller there. Figure 7 shows the scenario of setting the cavity resonating frequency f_R equal to $f_{\rm rf}$ at the ramp time of 13.33 ms.

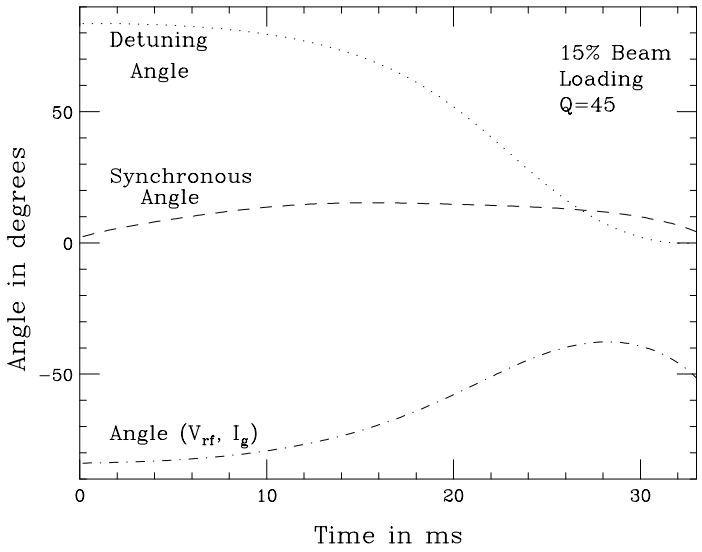

FIGURE 6. When the cavity resonant frequency is chosen as the rf frequency at the end of the ramp, both the detuning angle as well as the angle between the cavity gap voltage $\tilde{V}_{\rm rf}$ and the generator current $\tilde{I}_g$ are large.

There is a price to pay for this choice of f_R; namely, there will be Robinson phase instability for the second half of the ramp when the rf frequency is larger than f_R. The instability comes from the fact that, below transition, the particles with larger energy have higher revolution frequency and see a smaller real impedance of the cavity, thus losing less energy than particles with smaller energy. Therefore, the synchrotron amplitude will grow. In other words, the upper synchrotron sideband of the image current interacts with a smaller real impedance of the cavity resonant peak than the lower synchrotron sideband. However, since the loaded quality factor Q_L is not small, the difference in real impedance at the two sidebands is only significant when the rf frequency is very close to the cavity resonant frequency. Thus, we expect the instability will last for only a very short time during the second half of the ramp. The growth rate of the synchrotron oscillation amplitude has been computed and is equal to [6]

$$\frac{1}{\tau} = -\frac{i_{\rm im}\beta\omega_s(R_+ - R_-)}{2V_{\rm rf}\cos\varphi_s} \ , \tag{4.2}$$

where

$$R_+ - R_- = \mathcal{R}e\Big[Z_{\rm cav}(\omega_{\rm rf}+\omega_s) - Z_{\rm cav}(\omega_{\rm rf}-\omega_s)\Big] \ , \tag{4.3}$$

$i_{\rm im}$ is the image current, β is the velocity with respect to light velocity, $\omega_s/(2\pi)$ is the synchrotron frequency, and $Z_{\rm cav}$ is the longitudinal impedance of the cavity. We see from Fig. 7 that the growth occurs for only a few ms and the growth time is at least ~ 25 ms. The total integrated growth increment from ramp time 13.33 ms is $\Delta G = \int \tau^{-1} dt = 0.131$ and the total growth is $e^{\Delta G} - 1 = 14.0\%$ which is acceptable.

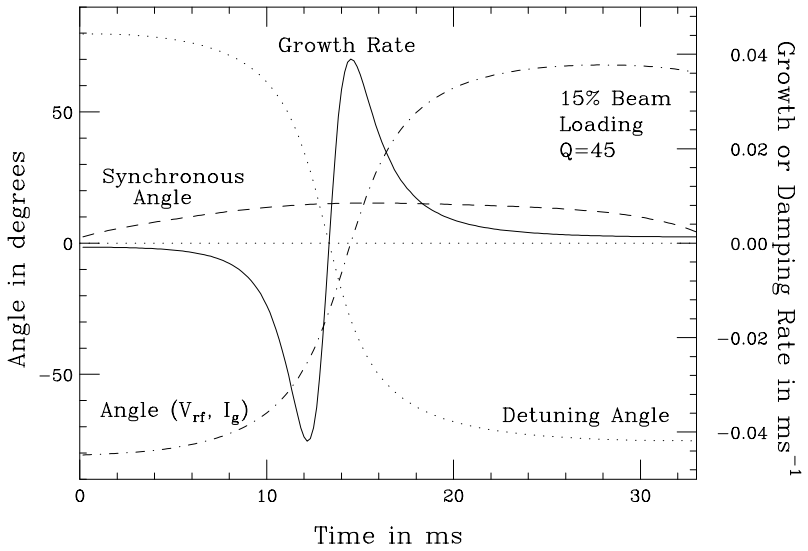

FIGURE 7. When the cavity resonant frequency is chosen as the rf frequency at the middle of the ramp at 13.33 ms, although the detuning angle as well as the angle between the cavity gap voltage $\tilde{V}_{\rm rf}$ and the generator current $\tilde{I}_g$ are large at both ends of the ramp, they are relatively smaller at the middle of the ramp where the gap voltage is large.

We also want to see whether Robinson's criterion for stable phase oscillation is satisfied for this rf consideration. For the second half of the ramp where the detuning angle $\psi < 0$, the phase is stable because we are below transition and the synchronous angle φ_s is between 0 and $\frac{1}{2}\pi$ (see Appendix B). For the first half of the ramp where $\psi > 0$, the sufficient condition for stability is the high-intensity Robinson's criterion:

$$\frac{i_{\rm im}}{i_0} < \frac{\cos\varphi_s}{\sin\psi\cos\psi} \ . \tag{4.4}$$

Figure 8 plots both sides of the criterion and shows that the criterion is well satisfied.

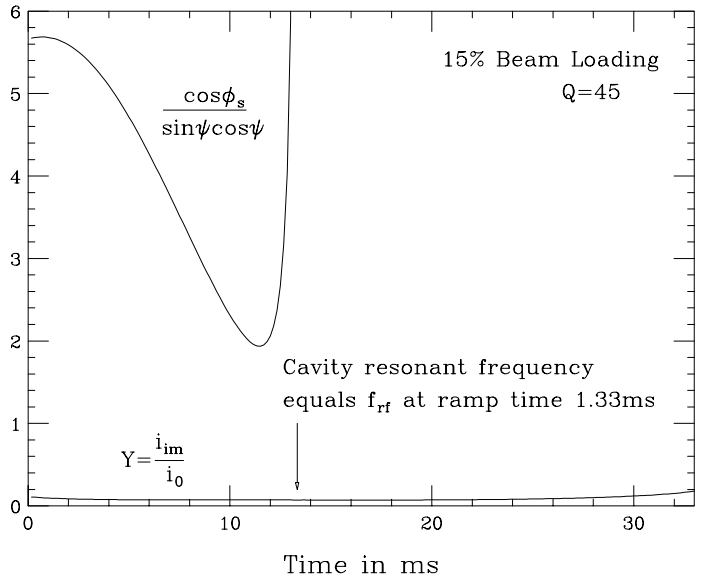

FIGURE 8. Plot showing the high-intensity Robinson's phase-stability criterion is satisfied.

V CONCLUSION

We started from a rf system designed by Griffin for the future Fermilab pre-booster with space charge slightly over-compensated and transient beam loading 85% compensated. Based on a resonant ramp curve with 3.75% second harmonic, we studied the possibility of having fixed-frequency non-tunable rf cavities. In order to reduce the phase angle between the rf voltage and the generator current, we proposed to set the resonant frequency of the cavity equal to the rf frequency at the middle of the ramp. Robinson phase instability would result in the second half of the ramp. The total integrated growth in synchrotron oscillation amplitude was found to be only $\sim 14\%$ which is small enough to be acceptable. We also checked that the whole ramp satisfies Robinson's high-intensity criterion for stable phase oscillation.

APPENDIX

In this appendix, we try to gather together the derivations of some of the formulas used in the paper. Most of them are well known. They are included here just for completeness.

A RF DETUNING

The rf cavity has a loaded shunt impedance R_s, a loaded quality factor $Q_{_L}$, and resonates at frequency $f_{_R} = \omega_{_R}/(2\pi)$. Corresponding to a beam particle revolving with frequency $f_0 = \omega_0/(2\pi)$, the rf frequency is $f_{\rm rf} = \omega_{\rm rf}/(2\pi) = h\omega_0$, where h is the rf harmonic. The impedance of the cavity seen by the particle at $f_{\rm rf}$ can be written approximately as

$$Z_{\rm cav} = \frac{R_s}{1 - jQ_{_L}\left(\dfrac{\omega_{_R}}{\omega_{\rm rf}} - \dfrac{\omega_{\rm rf}}{\omega_{_R}}\right)} \approx R_s \cos\psi \, e^{j\psi} \ , \tag{A.1}$$

where ψ is the rf tuning angle, which is defined as

$$\tan\psi = 2\,Q_{_L}\frac{\omega_{_R} - \omega_{\rm rf}}{\omega_{_R}} \ . \tag{A.2}$$

This detuning is necessary because (1) we want the load to appear real to the generator (the generator current i_g in phase with the cavity gap voltage $V_{\rm rf}$) so that there will not be any power reflection to the generator, and (2) both the generator voltage V_g and the beam-loading voltage $V_{\rm im}$ contribute to the cavity gap voltage. This is illustrated in the phasor diagram in Fig. 9, where the tilde represents a phasor rotating counter-clockwise with angular frequency $\omega_{\rm rf}$. Here, we assume most of the transient beam-loading has been cancelled; therefore, the image current phasor $\tilde{i}_{\rm im}$ has a magnitude much smaller than that of the beam current phasor $\tilde{i}_b$. According to Eq. (A.1), we see from Fig. 9 that both the beam-loading voltage phasor $\tilde{V}_{\rm im}$ and the generator voltage phasor $\tilde{V}_g$ are at a phase ψ ahead of their respective current phasors $\tilde{i}_{\rm im}$ and $\tilde{i}_g$. Since these two voltage phasors add up to give the gap voltage phasor $\tilde{V}_{\rm rf}$ which has a synchronous angle φ_s, we must have after dividing by $R_s\cos\phi$,

$$i_g \sin\psi = i_{\rm im}\sin(\tfrac{\pi}{2} - \varphi_s + \psi) \ . \tag{A.3}$$

Resolving the current contributions along $\tilde{i}_g$, we have

$$i_g = i_0 + i_{\rm im}\sin\varphi_s \ , \tag{A.4}$$

where $i_0 = V_{\rm rf}/R_s$ is the total current in phase with the cavity gap voltage. Eliminating i_g, we arrive at

$$\tan\psi = \frac{i_m\cos\varphi_s}{i_0} \ . \tag{A.5}$$

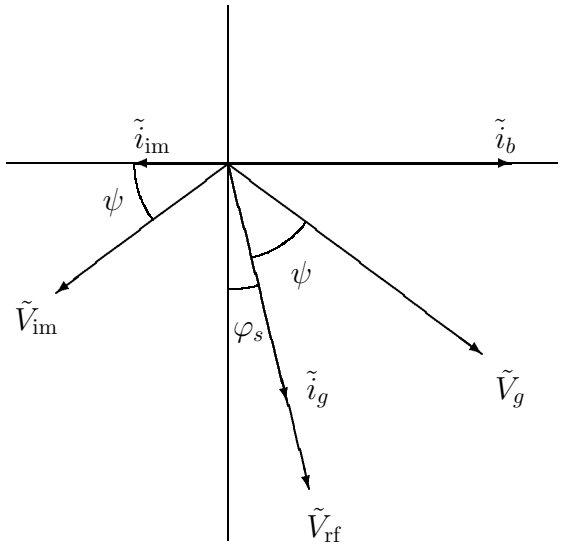

FIGURE 9. Phasor plot showing the vector addition of the generator voltage phasor $\tilde{V}_g$ and the beam-loading voltage phasor $\tilde{V}_{\rm im}$ to give the gap voltage phasor $\tilde{V}_{\rm rf}$ in a rf cavity. Note the detuning angle ψ which put the gap current phasor $\tilde{i}_g$ in phase with the gap voltage phasor.

B ROBINSON'S STABILITY CRITERIA

Now let us study the conditions for phase stability. Suppose that the beam particle has a slightly larger energy than the synchronous particle. After a revolution or h rf periods, $\tilde{i}_b$ in Fig. 9 will be ahead of the x-axis by a small angle $\epsilon > 0$ if it is below transition. Then the accelerating voltage it sees will be $V_{\rm rf}\sin(\varphi_s - \epsilon)$ instead of $V_{\rm rf}\sin\varphi_s$, or an extra decelerating voltage of $\epsilon V_{\rm rf}\cos\varphi_s$, and it receives less energy from the cavity than the synchronous particle. The motion is therefore stable. This is Robinson's criterion for establishing stable phase oscillation when beam loading can be neglected [5]. In other words, one requires

$$\begin{cases} 0 < \varphi_s < \frac{\pi}{2} & \text{below transition,} \\ \frac{\pi}{2} < \varphi_s < \pi & \text{above transition.} \end{cases} \tag{B.1}$$

When beam loading is included, the gap voltage phasor $\tilde{V}_{\rm rf}$ will be modified also, because the image current phasor $\tilde{i}_{\rm im}$ and hence the beam-loading voltage phasor $\tilde{V}_{\rm im}$ also advance by the small angle ϵ after h rf periods. The extra beam-loading voltage phasor is $\epsilon i_{\rm im} R_s \cos\psi\, e^{j(\psi+3\pi/2)}$. If $\psi < 0$, this phasor will point into the 3rd quadrant and decelerate the particle in concert with $\epsilon V_{\rm rf}\cos\varphi_s$, causing no instability. On the other hand, if $\psi > 0$, this phasor will point into the 4th quadrant and accelerate the particle instead. To be stable, the extra accelerating voltage on the beam must be less than the amount of decelerating voltage $\epsilon V_{\rm rf}\cos\varphi_s$, or

$$\frac{i_{\rm im}}{i_0} < \frac{\cos\varphi_s}{\sin\psi\cos\psi} \qquad \begin{cases} \psi > 0 & \text{below transition,} \\ \psi < 0 & \text{above transition,} \end{cases} \tag{B.2}$$

which is called Robinson's high-intensity criterion for phase stability. Satisfying this criterion just enables stable oscillating like sitting inside a stable potential well and there will not be any damping. Violating this criterion the particle will be in an unstable potential well so that phase oscillation will not be possible.

C TRANSIENT BEAM LOADING INCLUDING PREVIOUS PASSAGES

We follow closely the approach by Boussard [7]. Let the bunch spacing be h_b rf buckets or T_b in time. The cavity time constant or filling time is $T_f = 2Q_{_L}/\omega_{_R}$ and the e-folding voltage decay decrement between two successive bunch passages is $\delta_{_L} = T_b/T_f$. During this time period, the phase of the rf fields changes by $\Psi = \omega_{_R}T_b - 2\pi h_b$, which can also be written in terms of the detuning angle,

$$\Psi = (\omega_{_R} - \omega_{\rm rf})T_b = \delta_{_L}\tan\psi \ , \tag{C.1}$$

where Eq. (A.2) has been used. The transient beam-loading voltage left by the first passage of a short bunch carrying charge q is $V_{t0} = q/C$. The total beam-loading voltage V_t seen by a short bunch is obtained by adding up vectorially the beam-loading voltages for all previous bunch passages. The result is

$$V_t = \tfrac{1}{2}V_{\rm t0} + V_{\rm t0}(e^{-\delta_{_L}}e^{j\Psi} + e^{-2\delta_{_L}}e^{j2\Psi} + \cdots) \ , \tag{C.2}$$

where the $\frac{1}{2}$ in the first term on the right side is the result of Wilson's fundamental theorem of beam-loading, which states that a particle sees only one-half of its own induced voltage. It is worth pointing out that these voltages are not phasors or components at the rf frequency. They are vectors that contain components of all frequencies. The summation can be performed exactly giving the result

$$V_t = \frac{q}{C}\Big[F_1(\delta_{_L},\psi) + jF_2(\delta_{_L},\psi)\Big] \ , \tag{C.3}$$

with

$$F_1 = \frac{1-e^{-\delta_{_L}}}{2D} \ , \qquad F_2 = \frac{e^{-\delta_{_L}}\sin(\delta_L\tan\psi)}{D} \ ,$$
$$D = 1 - 2e^{-\delta_{_L}}\cos(\delta_L\tan\psi) + e^{-2\delta_{_L}} \ . \tag{C.4}$$

Notice that $\delta_{_L} \approx \pi h_b/Q_{_L}$, which is 0.0698 for $h_b = 1$ and $Q_{_L} = 45$. When the detuning angle $\psi = 0$, $|V_t| \approx V_{t0}/(2\delta_{_L})$. The functions F_1 and F_2 are computed at some other values of ψ, which are listed in Table 1 and plotted in Fig. 10.

We see that the total transient beam loading V_t falls rapidly as the detuning angle ψ increases. It vanishes approximately $\sim 88.7^\circ$ and oscillates rapidly after that. However, the choice of a large ψ is not a method to eliminate beam loading, because the steady-state beam loading will not be reduced.

TABLE 1. F_1 and F_2 for some values of the detuning angle ψ.

ψ	$\Psi = \delta_L \tan\psi$	F_1	F_2
0°	0°	$\sim \frac{1}{2\delta_L}$	0
84.9°	45°	0.061	1.197
87.5°	90°	$\sim \frac{\delta_L}{4}$	$\sim \frac{1}{2}$
88.7°	180°	$\sim \frac{\delta_L}{8}$	0

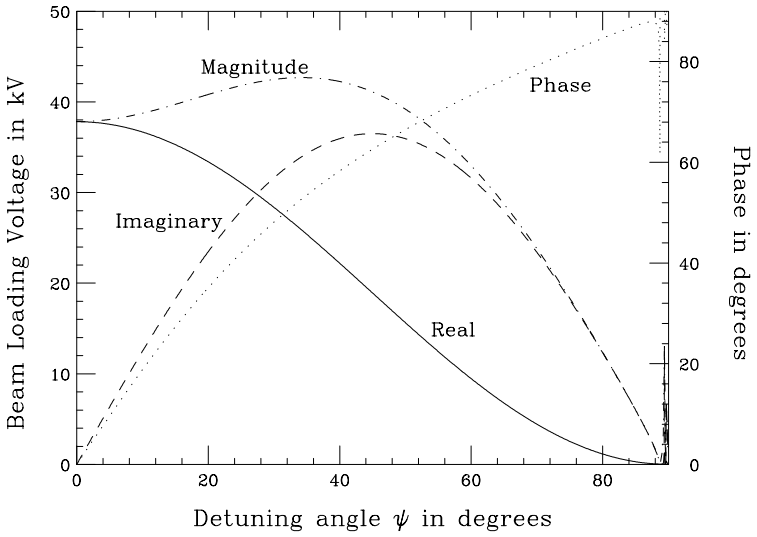

FIGURE 10. Plot of transient beam-loading voltage including all previous bunch passages, $\frac{q}{C}(F_1 + jF_2)$, versus detuning angle ψ.

REFERENCES

1. C. Ankenbrandt, these proceedings.
2. J.E. Griffin, *RF System Considerations for a Muon Collider Proton Driver Synchrotrons*, Fermilab report FN-669, 1998.
3. K.Y. Ng and Z.B. Qian, Proc. Phys. at the First Muon Collider and at Front End of a Muon Collider, Fermilab, Batavia, Nov. 6-9, 1997.
4. J.E. Griffin, K.Y. Ng, Z.B. Qian, and D. Wildman, *Experimental Study of Passive Compensation of Space Charge Potential Well Distortion at the Los Alamos National Laboratory Proton Storage Ring*, Fermilab Report FN-661, 1997.
5. P.B. Robinson, *Stability of Beam in Radiofrequency System*, Cambridge Electron Accel. Report CEAL-1010, 1964.
6. See for example, H. Wiedemann, *Particle Accelerator Physics II*, Springer, 1995, p.203.
7. D. Boussard, *Beam Loading*, Fifth Advanced CERN Accelerator Physics Course, Rhodes, Greece, Sep. 20-Oct. 1, 1993, CERN 95-06, p.415.